TECHNICAL MEMORANDUM

421

On the usage of screen-level parameters and microwave brightness temperature for soil moisture analysis

G. Seuffert, H.Wilker[1], P. Viterbo, M.Drusch, J.-F. Mahfouf[2]

Research Department

[1] MIUB, Germany, [2]SMC, Canada

submitted to J. Hydrometeor.

October 2003

European Centre for Medium-Range Weather Forecasts
Europäisches Zentrum für mittelfristige Wettervorhersage
Centre européen pour les prévisions météorologiques à moyen terme

For additional copies please contact

The Library
ECMWF
Shinfield Park
Reading
RG2 9AX
library@ecmwf.int

Series: ECMWF Technical Memoranda

A full list of ECMWF Publications can be found on our web site under:
http://www.ecmwf.int/publications/

Abstract

This study focuses on testing two different soil moisture analysis systems based on screen-level parameters (2m-temperature T_{2m}, 2m-relative humidity RH_{2m}) and 1.4 GHz passive microwave brightness temperatures T_B. First, a simplified Extended Kalman Filter (EKF) system is compared with an Optimal Interpolation (OI) method assimilating screen-level parameters in a single column version of the European Centre for Medium-Range Weather Forecasts (ECMWF) numerical weather prediction model. In the second part of this study, the EKF is applied to investigate whether the synergy of T_{2m}, RH_{2m} and additionally T_B in an assimilation framework improves the simulated soil moisture and atmospheric parameters.

For a summer period (130 days) during the First ISLSCP field Experiment (FIFE) 1987 it is shown that the OI and EKF analysis systems give similar results. Both systems distinguish consistently between periods of atmospheric and surface controlled fluxes. Though the overall soil water is adjusted by the same amount, the EKF-system simulates increments increasing from the first to the third layer whereas in OI method they are equally distributed.

The EKF system is applied for the Southern Great Plains field experiment 1997 (SGP97) testing the assimilation of a synergy of T_{2m}, RH_{2m} and T_B. The observed root zone soil moisture is best simulated by the control run and when T_B is assimilated. The assimilation of T_{2m} and RH_{2m} worsens the simulated root zone soil moisture compared with observations, because during a ten day period modeled T_{2m} and RH_{2m} considerably diverge from observations and soil moisture is tuned to compensate for deficiencies in the model. But in comparison with observed net radiation, heat fluxes and near-surface soil moisture it is shown that the assimilation of the synergy of observation types (T_{2m}, RH_{2m} and T_B) gives more consistent results than when they are assimilated separately.

1 Introduction

The need to realistically simulate soil moisture as a lower boundary condition in Numerical Weather Prediction (NWP) models has become widely acknowledged. Soil moisture is a key parameter in the interaction between land surface and atmosphere, which controls the partitioning of available energy in sensible and latent heat flux and hence boundary-layer and lower tropospheric conditions. But during NWP simulations considerable soil moisture drifts can be caused by a combination of erroneous precipitation and cloudiness predictions, which might also be triggered by misspecified soil moisture (Mölders and Raabe, 1997, Seuffert et al., 2002), and by imperfect parameterizations of soil processes and soil-atmosphere interactions.

Initialization of soil moisture with in-situ observations is not feasible, because no extensive observation network exists. Therefore, an incorporation of indirect observations providing information about soil moisture based on assimilation techniques is useful. Additionally, data assimilation takes into account the observation and model errors to create an optimal estimate of a smaller associated error. A number of studies explore the use of different observation types with various assimilation methods. Conventional data e.g. screen-level parameters (T_{2m},RH_{2m}) and satellite data e.g. radiometric surface skin temperature and passive microwave brightness temperature can be used to adjust soil moisture in an assimilation framework. In the following we distinguish their use with regard to the basic underlying physical process connecting the observation types and soil moisture: One category of studies (i) focuses on the assimilation of screen-level parameters like T_{2m}, RH_{2m} or radiometric surface heating rates (morning surface temperature tendency after sun rise). The second group (ii) uses L-band (1.4 GHz) or C-band (6.9 GHz) microwave brightness temperature observations T_B to adjust soil moisture.

(i) In atmospheric conditions with a strong surface-atmosphere coupling (e.g. low cloudiness, strong solar forcing, weak advection), screen-level parameters and surface temperature change over land are considerably controlled by the root zone soil moisture, because under these conditions the soil moisture content dominates the partitioning of available energy into latent and sensible heat flux and hence the amount of evaporative cooling at the surface. Therefore, a comparison of observed and simulated screen-level parameters or heating rates can be used to adjust simulated root zone soil moisture in an assimilation framework. Several studies have shown that the assimilation of screen level parameters based on Optimal Interpolation (OI), 1-dvar and Kalman Filter like

systems, prevented soil moisture drift and improved the simulation of T_{2m}, RH_{2m} and land surface energy fluxes (e.g. Mahfouf, 1991; Rhodin et al., 1999) . The assimilation of screen-level parameters is successfully realized in operational forecasts at e.g. European Centre for Medium-Range Weather Forecasts (ECMWF) (Douville et al., 2000), Météo France (Giard and Bazile, 2000), German Weather Service (DWD) (Hess, 2001) and Canadian Weather Centre (Bélair et al., 2003). The relationship between soil moisture and remotely sensed surface heating rates was investigated by Wetzel et al. (1984) and tested in assimilation frameworks by McNider et al. (1994), Jones et al. (1998a+b) and van den Hurk and The (2002). Compared with screen-level observations remotely sensed heating rates derived from IR measurements have the advantage of a more uniform data coverage but they can only be derived for cloud-free satellite pixels. For a case study, Margulis and Entekhabi (2003) have shown that the assimilation based on a variational approach of both screen-level parameters and radiometric surface temperature leads to more robust estimates than the assimilation of only one observation type.

(ii) The second group of studies investigates the assimilation of microwave brightness temperatures (1.4 and 6.9 GHz). At these frequencies T_B is influenced by soil moisture information of the near surface layer (a few cm), soil texture, actual soil moisture content, soil temperature profile, vegetation fraction and vegetation water content. In an assimilation framework this near surface soil moisture information has to be transported to the deeper root zone layers for simulating the impact on atmospheric parameters. Several studies have shown that this can be successfully achieved with assimilation algorithms like the Ensemble Kalman Filter, Extended Kalman Filter or variational algorithms (Reichle et al., 2001+2002; Margulis et al., 2002; Crow and Wood, 2003; Seuffert et al., 2003). So far 1.4 GHz T_B are only available for special field experiments or as synthetically produced data sets, but might become available in 2006 with the planned satellite missions Soil Moisture and Ocean Salinity (SMOS) mission (Kerr et al., 2001) and the Hydrosphere State Mission (HYDROS). The satellite programs Scanning Multichannel Microwave Radiometer (SMMR) and Advanced Microwave Scanning Radiometer - EOS (AMSR-E) carried/carry 6.6 and 6.9 GHz instruments, respectively, but they have a rather coarse horizontal field of view ($>50\text{km}^2$) and at these frequencies the vegetation influence is stronger than it is at 1.4 GHz.

The purpose of this paper is two-fold: (i) First, the performance of the OI method (operational at e.g. ECMWF) and a simplified Extended Kalman Filter (EKF) (operational at DWD) for soil moisture analysis based on T_{2m} and RH_{2m} are compared. Both systems are tested with the single column version (SCM) of the ECMWF model. The main difference between the two methods is the calculation of the forecast errors: In OI the forecast errors are fixed to statistically derived values whereas in EKF they evolve in the assimilation procedure depending on the weather regime. For comparison of the two methods, data from the First ISLSCP Field Experiment (FIFE) 1987 are used because the experiment covers a whole summer period and has a well established field data set (Betts and Ball, 1998).

(ii) The advantage of easy implementation for new observation types in the EKF system is exploited in the second part of this study. Seuffert et al. (2003) have shown that the combined assimilation of observed screen-level parameters and synthetically derived 1.4 GHz T_B observations gave promising results, when compared with observed gravimetric soil moisture and surface fluxes. Here, soil moisture analysis is based on screen-level parameters and brightness temperatures synergy with observed data for both data sources. The EKF method is applied to assimilate observed T_{2m}, RH_{2m} and T_B acquired during the 1997 Southern Great Plains Hydrology field experiment (SGP97) (Jackson et al., 1999) into the SCM.

The paper is organized as follows: First the basic characteristics of the SCM, land surface microwave emissivity model (LSMEM), and assimilation methods are described (section 1 and 2). The set of soil moisture experiments performed for the FIFE 1987 and SGP97 data sets is outlined in section 3. The results of the OI compared with the EKF method for FIFE87 and of soil moisture analysis with the synergy of T_{2m}, RH_{2m} and T_B for SGP97 are covered in section 4. Section 5 discusses the results and gives conclusions.

2 Models

2.1 Single Column Model

The use of a NWP for soil moisture analysis has the advantage that not only land surface related variables (e.g. T_B, surface skin temperature T_0) but also atmospheric parameters (e.g. T_{2m}, RH_{2m}) can be exploited for soil moisture analysis. Using a NWP the boundary layer acts as a reservoir replenished by surface heat and moisture fluxes while the fluxes are influenced by the underlying soil moisture. Therefore, background errors in T_{2m} and RH_{2m} can be used, under appropriate conditions, to initialize soil moisture. In this study the soil moisture analysis systems are tested with the SCM of the ECMWF model (cycle version CY23R4). The SCM is a hydrostatic model based on the primitive equations incorporating 60 atmospheric vertical levels with a well resolved boundary layer (lowest model level 10m above surface, and 8, 11,15, 17, and 22 levels below 500, 1000, 2000, 3000, and 5000 m, respectively). It uses a comprehensive physical parameterization package. The radiation scheme uses the shortwave code developed by Fouquart and Bonnel (1980) with cloud optical properties described in Morcrette (2002) and the longwave scheme uses a version of the Rapid Radiative Transfer Model (Mlawer et al 1997) described in Morcrette (2002). Turbulent heat and water transfer in the boundary layer are described in Beljaars and Viterbo (1998). The moist physical package, including convective and large-scale precipitation, is described in Gregory et al. (2000), and includes a modified version of the Tiedtke convection scheme (1989) and the prognostic cloud scheme of Tiedtke (1993), with the modifications of Jakob and Klein (2000).
The SCM incorporates a land surface model called TESSEL (Tiled ECMWF Scheme for Surface Exchanges over Land; Viterbo and Beljaars, 1995; van den Hurk et al., 2000). In TESSEL the soil processes are calculated in four layers (0.07, 0.21, 0.72 and 1.68 m) based on the Fourier diffusion law to solve the heat budget and Darcy's law for the vertical water transport. As boundary conditions at the bottom heat flux is set to zero and free drainage is assumed. The land energy balance is solved for six tiles (low and high vegetation, bare ground, high vegetation with snow beneath, snow on low vegetation, interception reservoir) separately with regard to skin temperature. In this study the weighted average skin temperature is used. Sensible and latent heat flux for each tile are parameterized by resistance based formulations. The total energy fluxes are given as the sum of the tiled energy fluxes weighted by their areal fractions. TESSEL considers 15 vegetation types with different characteristics (e.g. LAI, minimum stomatal resistance, vegetation coverage, root distribution).
The SCM is forced every 6 hours with vertical velocity, geostrophic wind vector, and advection of temperature, wind vector and specific humidity taken from the ERA40 atmosphere re-analysis. Every 24 hours the SCM is initialized by wind vector, temperature, surface pressure, specific humidity, specific cloud liquid and ice water contents and cloud fraction. In contrast to the usual application of the SCM, in this study soil moisture , soil and skin temperature run free to explore the influence of the soil moisture analysis schemes.

2.2 Land Surface Microwave Emissivity Model

The assimilation of brightness temperatures requires a radiative transfer model as observation operator. For the low frequency passive microwave spectral region the solution for the radiative transfer equation is well known. As outlined in Kerr and Njoku (1990) the brightness temperature for vegetated surfaces (T_{BV}) can be written as:

$$\begin{aligned} T_{BV} &= T_{au} + e^{-\tau_{at}}(T_{ad} + T_{sky}e^{-\tau_{at}})(1-\varepsilon)e^{-2\tau^*} + e^{-\tau_{at}} \\ &\quad \left[\varepsilon T_s e^{-\tau^*} + T_v(1-\omega^*)(1-e^{-\tau^*})(1+(1-\varepsilon)e^{-\tau^*})\right] \end{aligned} \quad (1)$$

where T_{au} and T_{ad} are the upward and downward emitted atmospheric radiation, T_s the soil temperature, T_v the vegetation temperature, T_{sky} the cosmic background radiation (2.7 K), ε the rough soil emissivity, and ω^* the effective single scattering albedo (Joseph et al. (1976)) of the vegetation. τ_{at} and τ^* are the optical depth of the atmosphere and the effective optical depth of the vegetation. The contribution from bare soils (T_{BS}) is given by:

$$T_{BS} = T_{au} + e^{-\tau_{at}}(T_{ad} + T_{sky}e^{-\tau_{at}})(1-\varepsilon) + e^{-\tau_{at}}\varepsilon T_s \quad (2)$$

TOA brightness temperatures originating from vegetated land surfaces and bare soil are computed separately and are combined linearly as a function of vegetation cover c:

$$T_B = (1-c)T_{BS} + cT_{BV} \quad (3)$$

For the sake of clarity we omit the notation for frequency and polarization dependency. However, it should be stressed that the parameters given in Eq. 1 to 3 (except from T_{sky}, T_s and c) depend on frequency and polarization. In this study, scattering in the atmosphere is neglected and T_{au} and T_{ad} are not polarization dependent. In the reviewed literature, a number of radiative transfer models based on Eq. 1 to 3 is available. They distinguish themselves through different parameterizations for the key components τ^*, ω^* and ε. In addition, depending on the frequency and the spatial resolution various assumptions on the individual parameters can be made to simplify Eq. 1 to 3. As an example, it can be assumed that the atmospheric contribution is constant at low frequencies (e.g. L-band). For high resolution measurements it may be valid to assume homogeneous field-of-views so that the fractional vegetation cover can be set to unity.

In assimilation studies the radiative transfer model has to be coupled to SVAT models. Consequently, a flexible interface should exist, which can cope with different numbers of soil layers at various depths and access the geophysical parameters used in the SVAT model. For observation system simulation experiments with synthetic data (e.g. Seuffert et al. (2003), Crow et al. (2001)) it is desirable to have different parameterizations for the same quantity to mimic uncertainties in the radiative transfer calculation and introduce observation errors. The model has been widely used in combined hydrological and remote sensing studies (e.g. Seuffert et al., 2003, Drusch et al., 1999; Drusch et al., 2001; Crow et al., 2001; Gao et al., 2003). Table 1 shows the different options for the LSMEM and the actual model set up for this study.

For a better understanding of the relation between the geophysical parameters listed in Table 2 and the active model components as given in Table 3 the most important parameterizations are introduced briefly. The dielectric model for the soil is an approximation of the Birchak model (Dobson et al., 1985). The expression for the dielectric constant of the wet soil η_m is given by:

$$\eta_m^\alpha = 1 + (\rho_b/\rho_s)(\eta_s^\alpha - 1) + m_v^\beta \eta_{fw}^\alpha - m_v \quad (4)$$

Table 1: LSMEM parameterization set up and options.

Parameter	Model set up	Option
Dielectric constant of saline water	Klein and Swift (1977)	-
Dielectric constant of wet soil	Dobson et al. (1985)	Wang and Schmugge (1980)
Smooth soil reflectivity	Fresnel Equations	Wilheit 1978)
Rough soil reflectivity	Wang and Choudhury (1981)	Wegmüller and Mätzler (1999)
Vegetation optical depth	Kirdyashev et al. (1979)	Wegmüller et al. (1995)
Vegetation single scattering albedo	constant	Wegmüller et al. (1995)
atmospheric effects (absorption by oxygen and water vapor)	Liebe (1989)	Liebe (1992)

Table 2: Vegetation and soil parameters for the LW02- site used in the LSMEM. Parameters were either measured (meas.), are taken from the literature (Lit.)(Dobson et al., 1985; Kerr and Njoku, 1990; Ulaby et al., 1983), were used to tune the LSMEM or were modeled.

Parameter	Value		Parameter	Value	
Vegetation coverage fraction	0.8	meas.	Soil water salinity	0.65 psu	meas.
Vegetation water content	0.8 g/cm^2	meas.	Soil dry bulk density	2.65 g/cm^3	meas.
Vegetation salinity	6.0 psu	Lit.	Soil clay fraction	20 %	meas.
Vegetation single scattering	0.1	meas.	Soil sand fraction	35 %	meas.
Vegetation structure coefficient	0.003	Lit.	Surface roughness	0.5 cm	tuned

where ρ_b and ρ_s are the soil bulk density and the soil specific density, respectively, m_v is volumetric soil moisture, η_s is the dielectric constant of the soil solids and η_{fw} the dielectric constant of free water. The constant α is set to 0.65 following Dobson et al. (1985). The soil texture dependent coefficient β is defined through the clay and sand fractions of the soil. The dielectric constant of free water is calculated from a modified Debye equation and depends on soil texture, frequency and salinity. For further details the reader is referred to Dobson et al. (1985). From η_m the smooth surface reflectivity r_s, which is polarization dependent, is calculated using the Fresnel equations. The reflectivity for rough surfaces $r_{r,p}$, which determines ε in equations (1) and (2) ($\varepsilon_p = 1 - r_{r,p}$), is calculated after Wang and Choudhury (1981):

$$r_{r,p} = (Qr_{s,q} + (1-Q)r_{s,p})e^{-hcos^2\theta} \tag{5}$$

Subscripts p and q indicate the different states of polarization, Q is the polarization coupling factor and θ the viewing angle. h is a function of frequency and surface roughness. The optical depth of the canopy layer can be written as (Kirdyashev et al., 1979):

$$\tau^* = AW_V \eta''_{sw} f/cos\theta \tag{6}$$

with the vegetation structure coefficient A, the vegetation water content W_V, frequency f and the imaginary part of the dielectric constant of saline water η''_{sw}, which depends on salinity and is calculated according to the parameterization published by Klein and Swift (1977).

2.3 Effective temperature for LSMEM calculation

The observed T_B is influenced by the soil temperature profiles, corresponding to the specific microwave penetration depth. The profile is not known in details, because generally soil models in NWP models have a coarse vertical resolution. Choudhury et al. (1982) proposed a formulation to account for the soil temperature profile using surface skin temperature T_0 and a deep soil temperature T_∞ (e.g. 0.5 - 1.3m) to calculate the effective temperature T_{eff}:

$$T_{eff} = T_\infty + (T_0 - T_\infty)\, C \tag{7}$$

The constant C depends mainly on the considered frequency. Here C is set to 0.246 for 1.4 GHz (Choudhury et al., 1982). When the surface temperature is not measured, observed air surface temperature is used instead of surface skin temperature. In this study we calculated T_{eff} based on T_∞ from layer 3 (0.64 m) for the simulations and for comparison with observed T_{eff} from 0.64 m which is available in the SGP97 data set.

3 Soil moisture Analysis Systems

In this study two soil moisture analysis systems are compared. The first one is the Optimal Interpolation (OI) algorithm operational at ECMWF (Douville et al., 2000), Météo France (Giard and Bazile, 2000) and Canadian Meteorological Centre (Bélair et al., 2003). The other data assimilation method, in this paper called 'simplified' Extended Kalman Filter (EKF), is based on the operational version implemented at DWD (Hess, 2001). Compared with the OI method the EKF system has the advantage that the forecast errors depend on the weather regime rather than being fixed to statistical derived values. Hence, atmospheric criteria for the applicability of the OI method are not necessary in the EKF method (Balsamo et al., 2003). Unlike OI, that can only use conventional observations at the standard times (00, 06, 12, 18 UTC), the EKF also allows to incorporate data , which are not available at these times (defined here as 'asynoptic' times), because it works on a 24h window. For these two reasons the EKF allows for an easier implementation of new observation types. In the second part of this study the EKF method is used to explore the potential of assimilating different observation types.

3.1 Optimal Interpolation Analysis

In OI the soil moisture of each layer (state vector **x**) is updated by a linear combination of the forecast errors of the screen-level parameters $T_{2m}$and RH_{2m} (observation vector **y**):

$$\mathbf{x}_a = \mathbf{x}_b + \mathbf{K}(\mathbf{y} - H(\mathbf{x}_b)) \tag{8}$$

where $\mathbf{x}_a$ and $\mathbf{x}_b$ are the analysis and background state vectors. H denotes the observation operator and **H** is the linearized H. In general, the gain matrix is given by:

$$\mathbf{K} = \mathbf{B}\mathbf{H}^{\mathrm{T}}[\mathbf{H}\mathbf{B}\mathbf{H}^{\mathrm{T}} + \mathbf{R}]^{-1} \tag{9}$$

where **B** and **R** denote the background and observation error covariances, respectively. In OI the gain coefficients are calculated by solving the system of linear equations (Eq. 9) minimizing the variance of the resulting analysis errors. When applied to the usage of T_{2m} and RH_{2m} for soil moisture analysis the elements of **K** for each soil layer j can be expressed as (Douville et al. 2000):

$$k_{j,T} = \frac{\sigma^b_{\eta_j}}{\Phi\sigma^b_T}\left\{\left[1+\left(\frac{\sigma^{obs}_{RH}}{\sigma^b_{RH}}\right)^2\right]\rho_{T,\eta_j} - \rho_{T,RH}\rho_{RH,\eta_j}\right\}F_1F_2, \tag{10}$$

$$k_{j,RH} = \frac{\sigma^b_{\eta_j}}{\Phi\sigma^b_{RH}}\left\{\left[1+\left(\frac{\sigma^{obs}_{T}}{\sigma^b_{T}}\right)^2\right]\rho_{RH,\eta_j} - \rho_{T,RH}\rho_{T,\eta_j}\right\}F_1F_2, \tag{11}$$

with

$$\Phi = \left[1+\left(\frac{\sigma^{obs}_{T}}{\sigma^b_{T}}\right)^2\right]\left[1+\left(\frac{\sigma^{obs}_{RH}}{\sigma^b_{RH}}\right)^2\right] - \rho^2_{T,RH}, \tag{12}$$

where η is the soil moisture content, σ^b and σ^{obs} represent the standard deviations of the background and observation errors, respectively, and $\rho_{x,y}$ are the correlation of the forecast errors between parameters x and y. For $\rho_{x,y}$ and σ^b the statistics were obtained using Monte Carlo method (Mahfouf 1991, Douville et al. 2000). The empirical functions F_1 and F_2 reduce the coefficient when solar incoming radiation is low (e.g. nighttime and cloudy days) and hence the interaction between soil and atmosphere is supposed to be lower. F_1 is a function of the solar zenith angle μ

$$F_1 = \frac{1}{2}(1 + tanh[7(\mu - 0.5)]) \tag{13}$$

and F_2 is a function of the solar transmittance T_r calculated from the downward solar radiation forecasted during the previous 6 h, $\overline{R_g}$:

$$T_r = (\frac{\overline{R_g}}{S_0 \mu})^{\mu} \tag{14}$$

$$F_2 = \frac{T_r - T_{rmin}}{T_{rmax} - T_{rmin}} \tag{15}$$

with S_0= solar constant, T_{rmin}= 0.2 and T_{rmax}=0.9 (Douville et al., 2000). The soil moisture analysis is also not applied in atmospheric conditions of strong wind speed ($>$ 10m/s), of low air temperature ($<$ 273.16 K), if the last 6-h precipitation exceeds 0.6 mm, and if there is snow on the ground. For comparison with the EKF analysis, the OI method is applied every 6 hours but the model is initialized only every 24 hours with six hourly forcing intervals. The 6h cycling and the F_1 function reduce the time when the analysis is applied in general to 06, 12 and 18 LST.

3.2 Simplified Extended Kalman Filter Analysis

3.2.1 Method

The analysis system called here 'simplified' EKF is based on the idea of minimizing the classical cost function J as in variational methods. Due to some assumptions outlined below (e.g. calculation of the observation operator) and updating of forecast error, it resembles an EKF.
The simulated soil moisture in the three root zone layers (state vector **x**) is improved by minimizing J by optimally combining the information from the model forecast of **x** and observed parameters (T_{2m}, RH_{2m}, T_B), specified in the observation vector **y**:

$$J(\mathbf{x}) = (\mathbf{x} - \mathbf{x_b})^{\mathrm{T}} \mathbf{B}^{-1} (\mathbf{x} - \mathbf{x_b}) + (\mathbf{y} - H(\mathbf{x}))^{\mathrm{T}} \mathbf{R}^{-1} (\mathbf{y} - H(\mathbf{x})) \tag{16}$$

Under the tangent linear hypothesis the minimum of J ($\nabla J = 0$) can be directly obtained rather than applying an iterative method (Hess, 2001). The solution for the analyzed state at time i is:

$$\mathbf{x_a}(i) = \mathbf{x_b}(i) + \mathbf{K}_{[i,i+24]} (\mathbf{y}_{[i,i+24]} - \mathbf{H}_{[i,i+24]} \mathbf{x}_{\mathbf{b},[i,i+24]}) \tag{17}$$

with the gain matrix:

$$\mathbf{K}_{[i,i+24]} = [\mathbf{B}^{-1}(i) + \mathbf{H}^T_{[i,i+24]} \mathbf{R}^{-1} \mathbf{H}_{[i,i+24]}(i)]^{-1} \mathbf{H}^T_{[i,i+24]} \mathbf{R}^{-1}, \tag{18}$$

where the $[i, i+24]$ indicates the 24h window. Here the gain matrix is expressed in model space rather than the usual formulation in observation space (see Eq. 9). Because the analysis is done on a 24-hour window, any control variable can be used from the time interval $[i, i+24]$. Assuming a quasi-linear problem close to the background state, H can be approximated by a one-side finite difference: One additional forecast run with initial perturbations is required for each state variable. H is calculated based on the difference between background and perturbed soil moisture of each layer and the difference of observed and modeled control variable at the time of the measurement. In this way, adjoint and tangent linear model are not needed. The background error covariance evolves temporally with a 24h cycling according to:

$$\mathbf{B}(i+1) = \mathbf{M}_{i \to i+24} \mathbf{A}(i) \mathbf{M}^T_{i \to i+24} + \mathbf{Q}(i) \tag{19}$$

where **Q** is the model error covariance matrix and **M** is the tangent linear of the forecast operator M. We assume that the observation and model errors are mutually uncorrelated and white. **A** is the analysis error covariance calculated by:

$$\mathbf{A}(i) = [\mathbf{H}^T_{[i,i+24]} \mathbf{R}^{-1} \mathbf{H}_{[i,i+24]} + \mathbf{B}^{-1}(i)]^{-1}. \tag{20}$$

In contrast to the original algorithm, described by Hess (2001), we account for the soil water transfer between the soil layers by using perturbed model runs to estimate **M**. The start values of x_b for the following day (i+24h) are calculated by:

$$\mathbf{x_b}(i+24) = M_{i \to i+24}\mathbf{x_a}(i) \tag{21}$$

3.2.2 Estimation of the model error

Q is assumed to be diagonal and constant in time. It was calculated as follows: Assuming an optimal analysis, it can be shown (Fisher, 2002) that:

$$\mathbf{R} - \overline{(\mathbf{y} - \mathbf{H}\mathbf{x}_a)(\mathbf{y} - \mathbf{H}\mathbf{x}_b)^T} = 0. \tag{22}$$

Consequently, for a sub-optimal analysis, that tends to draw too closely to the background, the expression in Eq. 22 will tend to be lower than zero. Conversely, the expression will tend to become greater than zero for a sub-optimal analysis that draws too closely to the observations. A number of case studies was performed with varied model and observation error covariances. It was found that a standard deviation of 0.005 m^3/m^3 for all three soil layers gave the best agreement between **R** and $\overline{(\mathbf{y} - \mathbf{H}\mathbf{x}_a)(\mathbf{y} - \mathbf{H}\mathbf{x}_b)^T}$ according to Eq. 22. This choice also resulted in reasonably small soil moisture increments.

3.2.3 Application

The analysis is applied on a 24 hour window with a start point at local midnight . The OI system has to be applied at the times when observation are available (e.g. times of the standard observation times), whereas in the EKF system data from the 24- assimilation window can be used. This allows for more flexible choice of observation times and especially observations from asynoptic times can be additionally used. For a fair comparison between OI and EKF system with the FIFE data set T_{2m} and RH_{2m} are assimilated at 06, 12 and 18 LST. To test the synergy of screen-level parameters and T_B with the EKF-system for the SGP97 data set, we take advantage of the flexibility of this system and assimilate T_B from 11 LST and T_{2m} and RH_{2m} from 09, 12 and 15 LST because around local noon the soil moisture- T_{2m} and RH_{2m} dependence is highest. T_b was measured around 11 LST at the considered field sites (section 4.1.2). The impact of the different observation types is partly determined by the corresponding observation and model error. The experiments are based on quality controlled observation data. Hence, observations errors can be assumed to be small and their standard deviations are set to 2K for T_{2m}, 10% for RH_{2m} and 2K for T_B. Additionally, the SCM is forced with quality controlled precipitation and incoming radiation. Consequently, the model error can be assumed to be rather small (section 3.2.2). For operational applications with erroneous forcing data sets larger model and observation errors should be chosen. For the calculation of the observation operator based on finite differences soil moisture is perturbed by a factor of 0.00001. Compared with Balsamo (2003) and Hess (2001) this choice is rather low but in this way non-linearities are avoided in our investigations. In this study for both algorithms horizontal correlations have been neglected.

4 Application

4.1 Observations

4.1.1 FIFE

The two assimilation methods are compared for data from the First ISLSCP Field Experiment (FIFE). Observations were made on a 15km $\times$ 15km site in the Konza prairie, Kansas (39°05'N, 96°53'W). The data set was prepared by Betts and Ball (1998) for the period 1.6 –9.10.1987. This data set consists of near-surface atmospheric parameters (e.g. T_{2m}, RH_{2m}, precipitation), and radiative forcing averaged over measurements from 10 stations in the field to get a single data set representative for FIFE. The heat fluxes were measured by eddy-correlation stations during four intensive field campaigns and estimated by the Bowen ratio method outside these campaigns (4-6 stations). They were also aggregated to a single data set. Additionally, the soil was monitored by profiles of soil moisture (gravimetric and neutron probe techniques) and temperature. The soil moisture observations are available on a daily basis during the intensive observation periods (IOP) and on a weekly basis outside the campaigns. Vegetation and soil parameters used in the model for FIFE are listed in table 3.

4.1.2 SGP97

To test the synergy of different observation types, data from the SGP97 experiment (18 June to 17 July 1997) are used (Jackson et al. 1999). This field campaign combined L-band brightness temperature observations from aircraft with a large variety of ground measurements taken at more than 40 sites within three investigation areas in Oklahoma, namely the Central Facility near Lamont, the Grazinglands Research Lab at El Reno and the Little Washita River watershed. A detailed description of the field experiment can be found in Jackson et al. (1999). This paper focuses on the Little Washita observation sites.

Table 3: Vegetation and soil parameters for the FIFE and LW02- site used in the land surface model.

Parameter	FIFE	SGP97
High vegetation type	Interrupted forest	Interrupted forest
High vegetation cover	0.07	0.03
Low vegetation type	Tall grass	Tall grass
Low vegetation cover	0.93	0.97
Roughness length for momentum	0.51	0.31
Roughness length for heat	0.016	0.026
Wilting point	0.353 m^3/m^3	0.26 m^3/m^3
Field capacity	0.201 m^3/m^3	0.11 m^3/m^3
Specifications of vegetation types:	Interrupted forest	Tall grass
minimum stomata resistance	175 s/m	100 s/m
LAI	2.5	2
Vegetation coverage	0.90	0.70

Site LW02 in SGP97 is situated in the north-east (34°57'N, 97°58'W, 370 m altitude) of the Little Washita watershed. On this particular site a long-term flux monitoring site was operated by the Atmospheric Turbulence and Diffusion Division (ATDD) of the US National Oceanic and Atmospheric Administration (NOAA) (Meyers, 2001) from 1996 until 1998. This flux monitoring station provides half-hourly observations of air temperature, relative humidity, wind speed and direction at 2 m height, near-surface air pressure, precipitation, incoming shortwave and net radiation, surface temperature, soil temperature at 6 depths between 2 and 64 cm, volumetric water content at 10 cm depth and fluxes of soil, sensible and latent heat. The surface flux values used for verification purposes were corrected by the University of Wisconsin-Madison to close the energy balance. Measured net radiation was adjusted for wind effects and calibrated with a Kipp and Zonen net radiometer. Additionally, it was assumed that the eddy correlation system accurately measured the Bowen ratio B. The corrected values of sensible heat flux H and latent heat flux LE were then calculated by $LE = \frac{R_{net}-G}{1+B}$ and $H = R_{net} - G - LE$ where R_{net} is the corrected net radiation and G is the site-averaged soil heat flux. Relative humidity was corrected down by 7% because of a bias in the original dataset (Meyers 2003). Missing incoming longwave radiation was filled with data taken from ECMWF 6-hour-forecasts that were initialized by ERA-40 re-analyses. As additional verification information data from a Soil Heat and Water Measurement System (SHAWMS) station of the US Department of Agriculture (USDA) Agricultural Research Service (ARS) were available. It provides soil water matrix potential values at six depths between 5 and 60 cm from which volumetric soil moisture was derived according to van Genuchten (1980). Soil and vegetation parameters used in the land surface model and for the LSMEM are listed in table 3 and 2.
Observations of 1.4 GHz brightness temperatures were provided by the Electronically Scanned Thinned Array Radiometer (ESTAR) (Le Vine et al., 1994) , which was mounted on aircraft flying at a constant height of 7.5 km. The brightness temperature observations were processed to a surface resolution of about 800 m and renormalized to nadir. Flights have been carried out from 18 June to 17 July in 1997 covering an area of 40 x 280 km. Theoretically every site was overflown once a day but because of technical problems and weather conditions no ESTAR data were available on the following days: 21–24 June, 28 June, 4–10 July and 15 July (Jackson et al., 1999).
Gravimetric soil moisture values were acquired between 18 June and 16 July. They were derived from samples of the upper 5 cm soil layer taken once every day. For this study the gravimetric soil moisture is converted to volumetric values with the soil bulk density specified in Table 2. No soil moisture data were available on 23 June and 26 June as well as on 4 July.

4.2 Experiment design

To compare the performance of OI and EKF method, a set of three model runs is conducted for the FIFE site: a control run without any soil moisture analysis and model runs in which the soil moisture is adjusted either by OI or EKF method assimilating T_{2m} and RH_{2m}. The SCM is forced every 20 min (model time step) with interpolated observations of precipitation, incoming solar and longwave radiation to avoid errors in the forcing crucial for soil moisture. The initial soil moisture conditions for all three model runs at 1 June 1987 are set to the observed values. All three model runs were started at midnight. The model runs are initialized every 24 hours and forced every 6 hours with atmospheric re-analysis (ERA40) data (section 2.1). In the OI system the analysis is performed every 6 hours whereas the EKF-system has a 24h cycling. Both systems assimilate data at 06, 12 and 18 LST (section 3.2.3).
The effect of combining screen-level parameters and microwave brightness temperature for soil moisture analysis is tested with the SGP97 data set. Two sets of experiments were performed for this investigation. The first type of experiment is done under perfect forcing conditions, which means the SCM is forced with observed precipitation, incoming shortwave and longwave radiation. The second type of experiments is performed under conditions in which precipitation is set to zero. This experiment shows whether the assimilation of T_{2m}, RH_{2m}

and/or T_B improves accuracy of modeled soil moisture and atmospheric parameters in case of erroneous specified forcing. For both type of SGP97 experiments four model runs are conducted: The first one is a control run without soil moisture analysis but with free running of soil moisture and soil temperature (Ctrl). In the KTR runs T_{2m} and RH_{2m} are assimilated and in the KB runs T_B is assimilated. In the fourth model run (KTRB) all three observation types T_{2m}, RH_{2m} and T_B are assimilated. All the model runs were started at local midnight and are reinitialized every 24 hours with atmospheric re-analysis (ERA40) data. The initial soil moisture conditions for all four model runs at 15 June 1997 are set to the observed values. For the assimilation, T_{2m} and RH_{2m} are taken from 09, 12 and 15 LST and T_B from 11 LST (section 3.2.3).

4.3 The information content of observations

In this study soil moisture analysis is based on screen-level parameters and T_B observations. In appropriate conditions (defined below) soil moisture content dominates the partioning of available energy into heat and moisture fluxes. These fluxes replenish the boundary layer reservoir and hence have a strong impact on screen-level parameters. Therefore, this indirect link between screen-level parameters and soil moisture through evaporative cooling can be used in soil moisture analysis. The assimilation method has to sufficiently distinguish between situations of weak and strong influence of soil moisture on screen-level parameters where the impact is high with strong solar forcing, weak advection, low vegetation coverage.
On the other hand the microwave T_B data contain a more direct information of the near surface soil moisture (few cm) and are less influenced by atmospheric conditions. The originating depth of the T_B signal depends on soil texture, soil temperature profile, vegetation fraction and vegetation water content additionally to soil moisture. In an assimilation framework the soil moisture information included in T_B observation has to be transported to the deeper layers in order to significantly change water content in the soil and hence have an impact on the overall hydrological budget.

5 Results

5.1 Comparison of OI and EKF assimilation schemes

The OI and EKF systems are tested for FIFE site (Betts and Ball, 1998). The main difference between OI and EKF system concerns the calculation of the forecast errors. Figure 1 shows the temporal evolution of the gain matrix **K** represented by the Froebenius norm (FN)

$$||FN|| = \sqrt{\sum_{l=1}^{3}\sum_{m=1}^{6}(k_{lm}^2)} \tag{23}$$

with l and m indexing the number of soil layers and observations, respectively. In general, FN of OI and EKF method evolves similarly (Fig.1), which leads to a similar evolution of the soil moisture increments compared with OI (Fig. 2). Both systems distinguish consistently between clear-sky and cloudy as well as precipitation periods in which the fluxes and hence screen-level parameters are strongly and weakly influenced by soil moisture, respectively (see Fig.1 of Douville et al, 2000 for development of precipitation and incoming solar radiation for FIFE). The OI system adjusts to the atmospheric conditions due to the carefully chosen atmospheric criteria whereas in EKF the forecast errors directly depend on the atmospheric conditions and no atmospheric criteria are applied. The FN of the EKF system is larger in clear-sky conditions than FN of OI, which means that the EKF method has a slight preference for the observations rather than the background. This results in

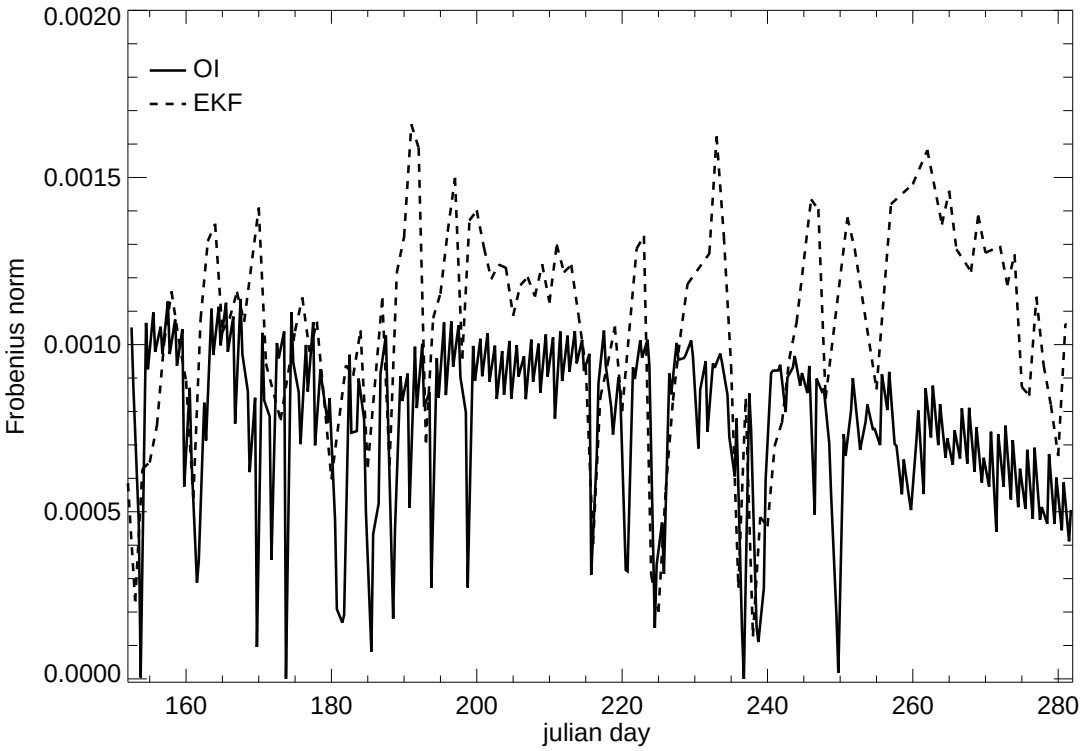

Figure 1: Evolution of the Froebenius norm of the gain matrix for the OI and EKF analysis system (1.6 – 9.10.1987).

slightly larger soil moisture increments (Fig.2).
The EKF system puts slightly more weight on the T_{2m} observations compared with the OI method for which the RH_{2m} gain elements are larger (not shown). Also in the OI system the weights for the three soil layers are almost the same whereas in the EKF system more weight is put on the third and second soil layer. This is a result of taking the water transport between the soil layers into account when updating the forecast errors. It ensures that the influence of any soil layer is not overestimated and it should lead to soil moisture increments of all three layers with the same sign at each analysis time step (Fig.2). The different weighting of each soil layer leads to increasing soil moisture increments from the first to the third soil layer whereas the soil moisture increments given by the OI system are similar for all 3 layers as shown in Figure 3. Larger corrections of the lower root zone layers are in agreement with the finding that errors are more persistent in these layers. At the end of the period (days 255 – 280) FN of EKF is large while the FN of OI decreases due to the effect of $F_1(\mu)$ criteria. Theoretically, the EKF system should detect a lower sensitivity because of the lower incoming solar radiation in this period. In this case the modeled T_{2m} is biased low whereas there is no clear bias in RH_{2m} leading to a considerable sensitivity and hence larger soil moisture increments. Unless the background field is improved the $F_1(\mu)$ criterion should be applied for the EKF system to avoid large soil moisture increments in winter.

Over spring to summer the hydrological role of the land surface scheme is to partioning correctly precipitation into evapotranspiration, runoff and soil water deficit. Figure 4a illustrates that the ctrl-run persistently underestimates evapotranspiration and overestimates soil moisture depletion, highlighting deficiencies in the model hydrological budget. When T and RH are assimilated the amount of evapotranspiration slightly increase whereas the soil moisture depletion increases in the period 170 – 195 and decreases at the end of the period

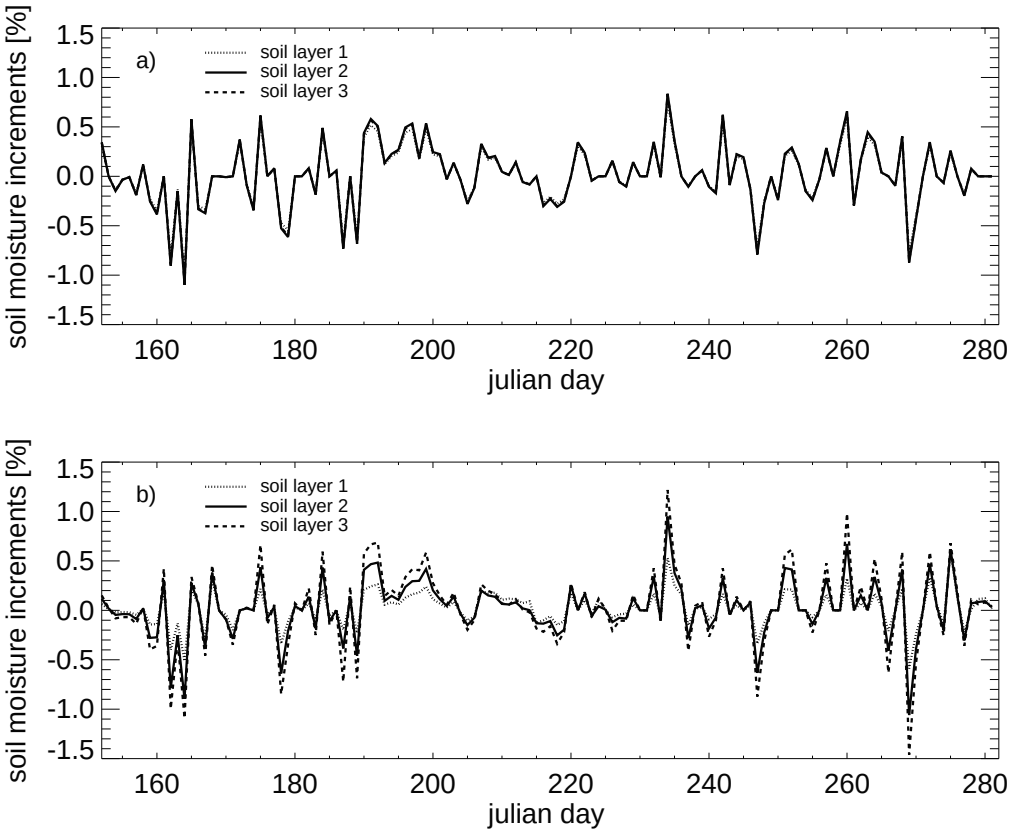

Figure 2: Evolution of the volumetric soil moisture increments given by a) OI and b) the EKF analysis system from 1.6–9.10.1987 for FIFE.

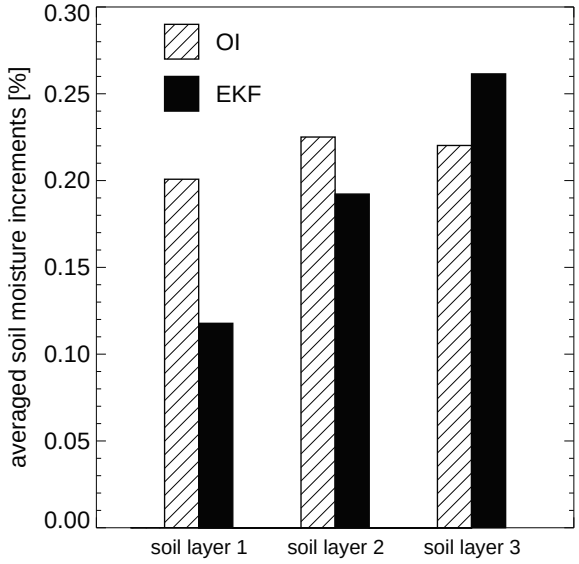

Figure 3: Comparison of the averaged volumetric soil moisture increments over 130 days (FIFE87) for each soil layer derived by OI and EKF analysis system

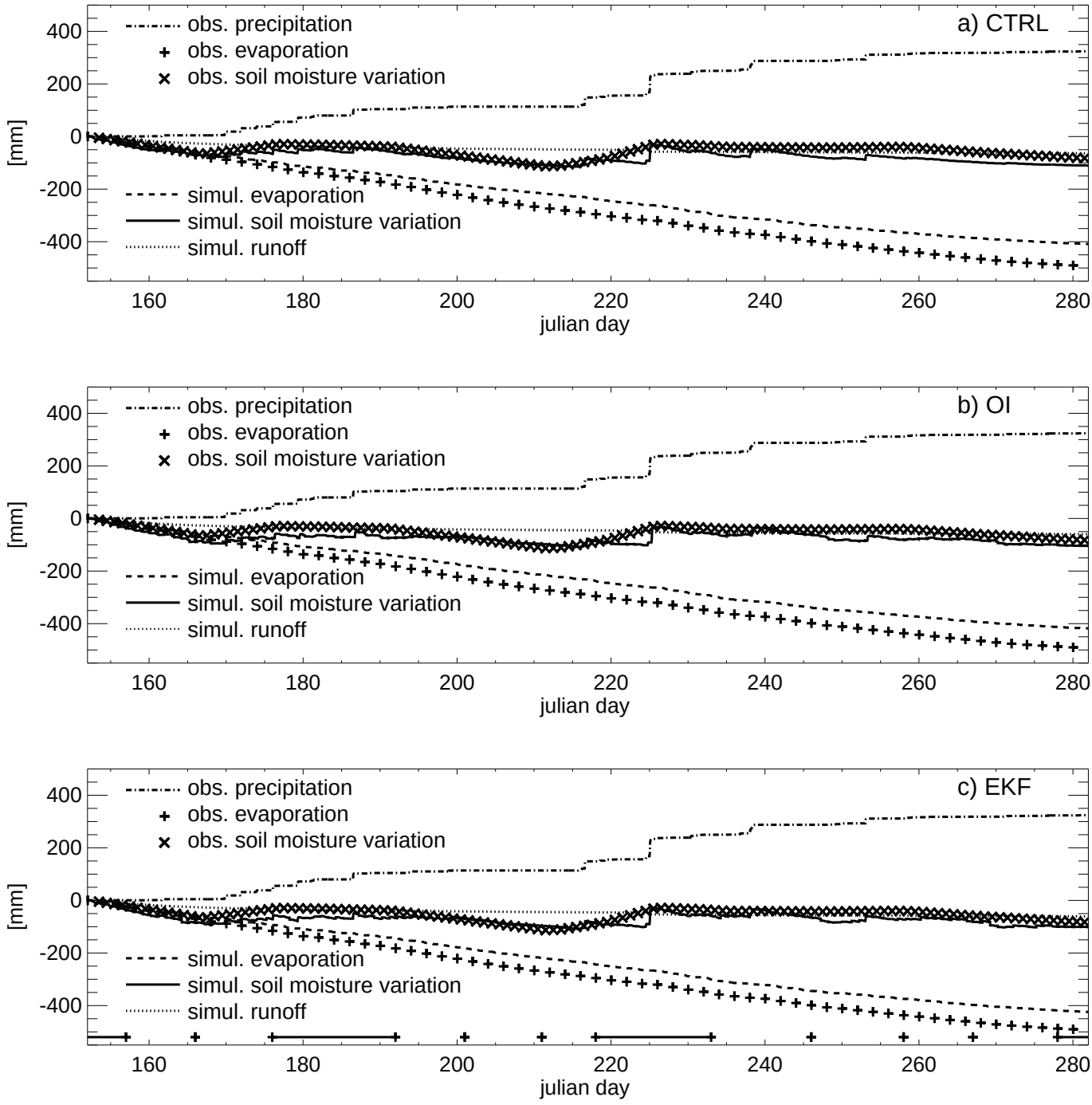

Figure 4: Time-integrated hydrologic budget simulated by a) the Control run, b) model run with OI and c) with EKF soil moisture analysis from 1.6 to 9.10.1987 for FIFE. In the lowest panel the IOP (daily soil moisture measurements) are indicated by lines and weekly soil moisture measurements are indicated by '+' (section 4.1.1).

(days 225–265). So the assimilation slightly compensates for problems in the model (Fig. 4b+c). The similar soil moisture increments calculated by the OI and EKF methods lead to similar results in the hydrological budget.

5.2 Synergy of T_{2m}, RH_{2m} and T_B for soil moisture analysis

In this section the synergy of T_{2m}, RH_{2m} and T_B is tested with EKF for SGP97 because this data set contains both observed T_{2m}, RH_{2m} and T_B and for comparison gravimetric soil moisture and heat flux measurements.

5.2.1 Alternative T_{eff} parameterizations

We investigate the effect of using different soil temperature parameterizations on T_B in the LSMEM calculations. Therefore, three model runs without any data assimilation were conducted: The first uses simulated soil temperature at 0.07m T_{7cm} and the second and the third one calculate T_{eff} (according to Eq. 4) where T_0 is either the 2m-air temperature or the surface skin temperature. Figure 5 shows that equation (4) improves the simulated T_B compared with the measured one. Using T_{eff} instead of T_{7cm} leads to differences of up to 6K, whereas the use of 2m air temperature or surface temperature in the calculation of T_{eff} only slightly (up to 1K) influences simulated T_B. Considering that a change of 2K in T_B results in a derived soil moisture change of about 0.01m^3/m^3, the influence of the soil temperature profile in the LSMEM calculations can not be neglected in the following data assimilation experiment with the setup for model and observation errors described in section 3.2.3. Therefore, T_{eff} according to Eq. 4, based on T_0 being the surface skin temperature, was used for the assimilation experiments.

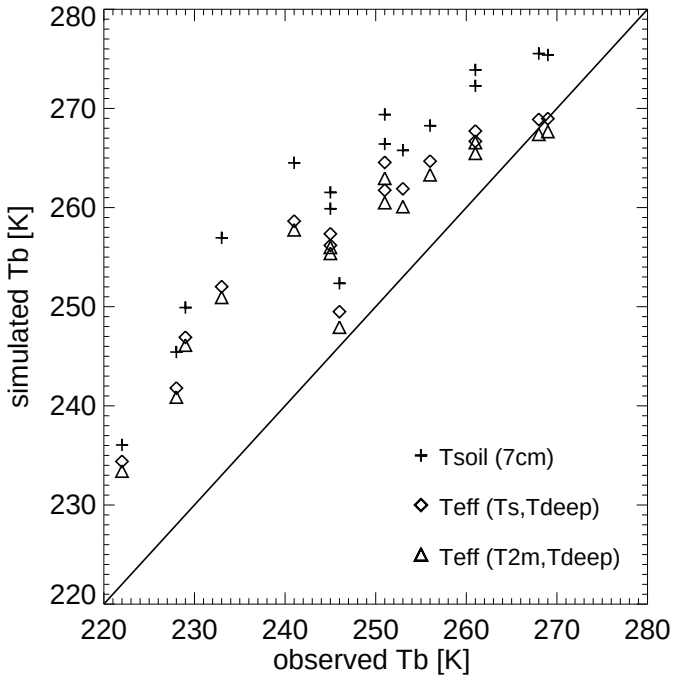

Figure 5: Scatterplot of observed versus simulated T_B with different parameterizations for the surface temperature in the LSMEM calculation for SGP97.

5.2.2 Fit to observed screen-level parameters and brightness temperature

Figures 6a,b and 7a show the daily mean temporal evolution of the assimilated parameters T_{2m}, RH_{2m} and T_B for the four simulations in comparison with the observations. All four model runs underestimate daily mean RH_{2m} and overestimate daily mean T_{2m}. As expected the simulation of T_{2m} and RH_{2m} is considerably improved in the KTR and KTRB runs. But also the assimilation of the independent parameter T_B results in a better agreement of simulated and observed T_{2m} and RH_{2m}, especially in the period 17.– 30.6. (days 169-181) and 12.–16.7. (days 194-198). In general, the best results are achieved when all three parameters are assimilated (see bias, RMS in Fig. 6a,b), because problems with one observation type (e.g. missing data) are compensated by the other type or the signals intensify each other (e.g. days 169-174, 181-192).
Especially in the period 173 –183 julian days all four model runs simulate a considerably drier and warmer boundary layer compared with the observations. Additionally, the simulations overestimate the multi-day variability of relative humidity. The problem seems to be related to the SCM-setup, which does not capture shallow convection. In contrast, the ERA40 data agree better to the observations (not shown). Figure 7a shows that in general the four model runs overestimate observed T_B because of an underestimation of surface soil moisture (Fig. 7b). The assimilation of T_{2m} and RH_{2m} already slightly reduces simulated T_B. The KB and KTRB runs capture observed T_B best. Especially at the beginning of the case study the bias between Ctrl- run and observations is considerably reduced (up to 10K).

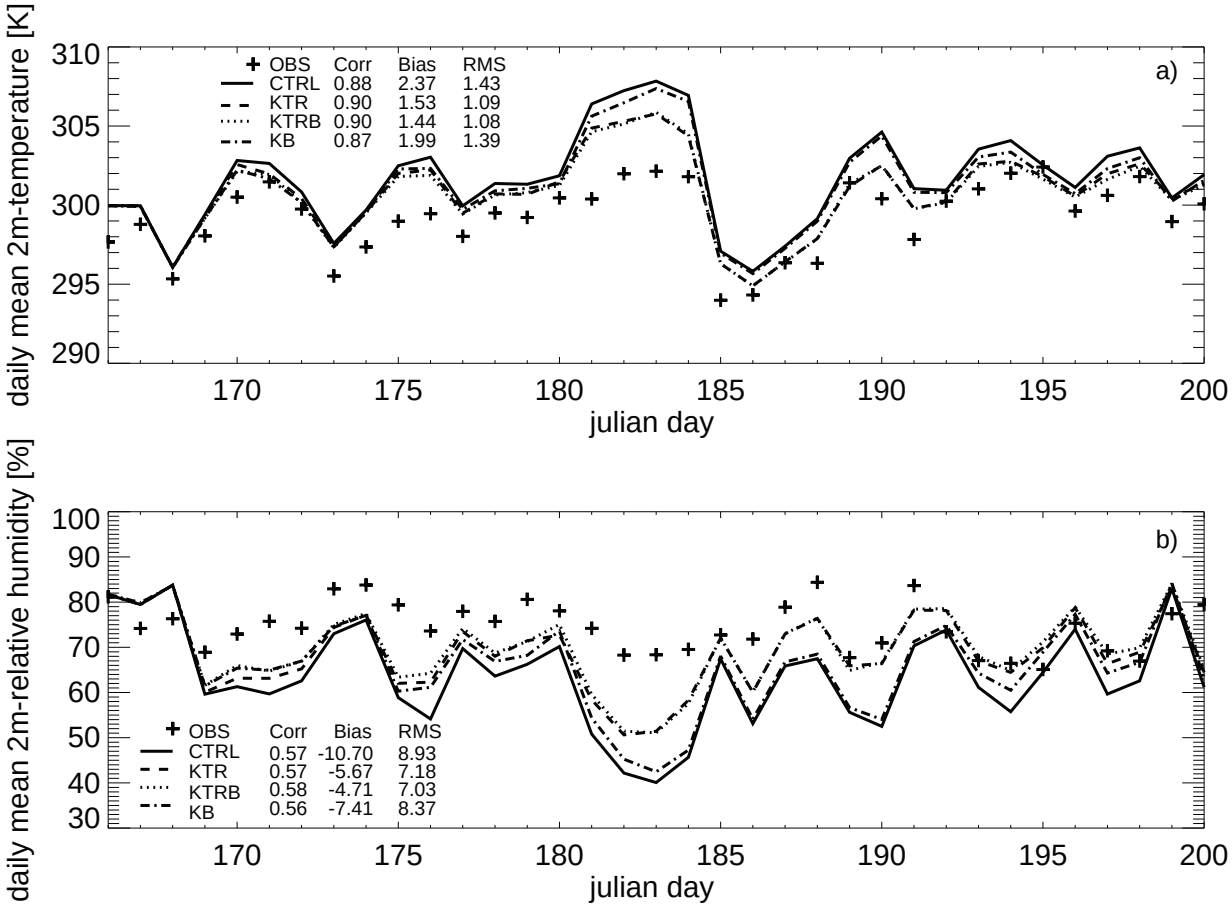

Figure 6: Temporal evolution for 15.6 – 19.7.1997 of a) 2m-temperature and b) 2m-relative humidity simulated by the ctrl-, KTR-, KB- and KTRB-run in comparison with observations from SGP97.

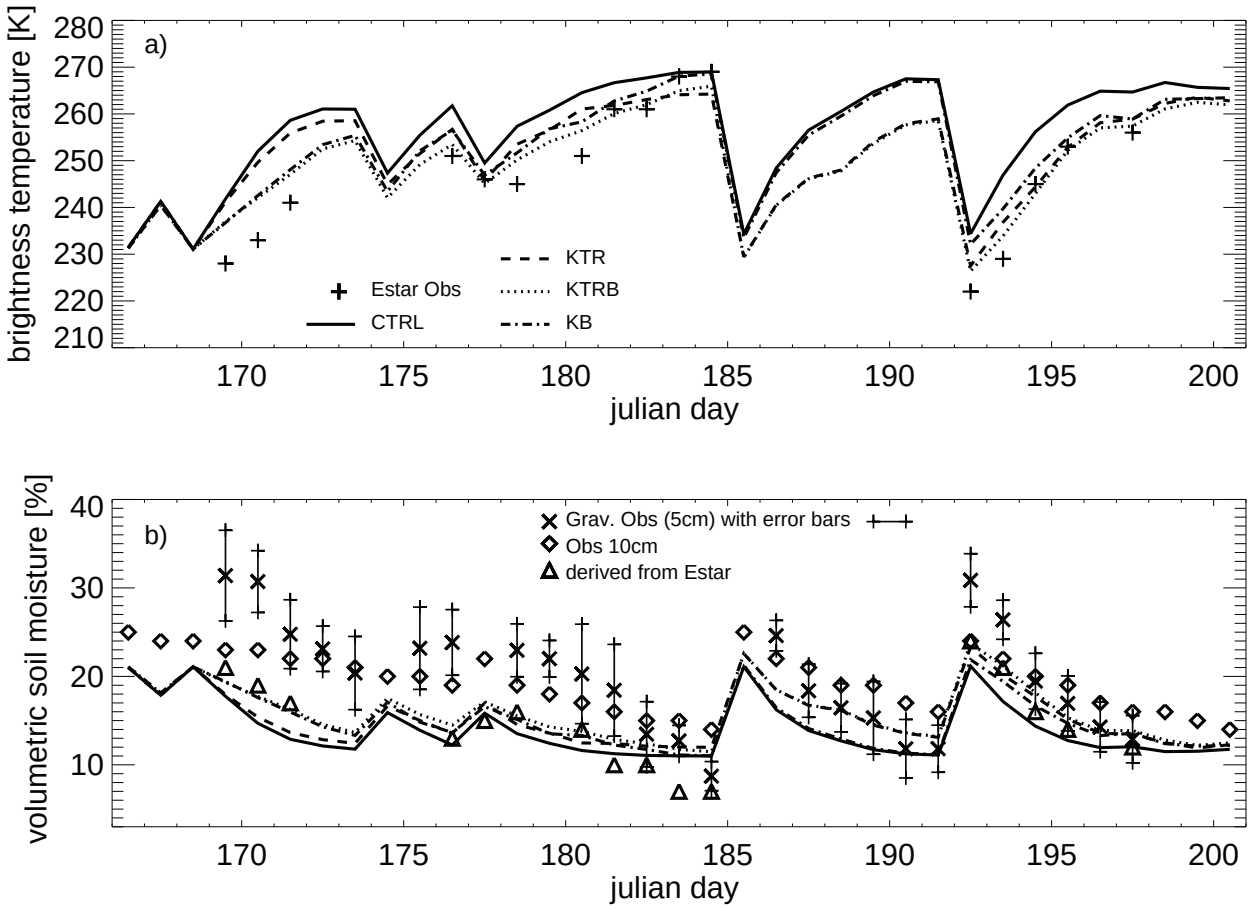

Figure 7: Temporal evolution for 15.6 – 19.7.1997 of a) 1.4 GHz microwave brightness temperature and b) surface soil moisture simulated by the ctrl-, KTR-, KB- and KTRB-run in comparison with observation from SGP97.

5.2.3 Fit to observed soil moisture

The root zone soil moisture is best captured by the control- and the KB-run (Fig. 8). The Ctrl-run slightly underestimates and the KB-run overestimates soil moisture. But both are still within the assumed error of the soil moisture observations. In the KTR and KTRB-runs water is added to the soil in the period 174 to 184 julian days though no precipitation was observed. This means that soil moisture is used to compensate for non soil moisture related deficiencies in the experiment setup. These deficiencies could be: (i) The model does not capture the observed evapotranspiration, because of deficiencies in the parameterization. (ii) The observed colder and moister atmosphere (Fig. 6a+b) compared with the simulations is not the result of higher root zone soil moisture values but is forced by atmospheric processes (e.g. advection), which are not captured by the SCM (section 5.2.2).

The observed surface soil moisture is captured best when T_{2m}, RH_{2m} and T_B are assimilated because in the period 185-192 julian day the assimilation of T_{2m} and RH_{2m} compensates for the missing T_B data (see Figure 7a) and the assimilation of T_B contains a more direct signal on the surface soil moisture (e.g. period 169-174 julian day).

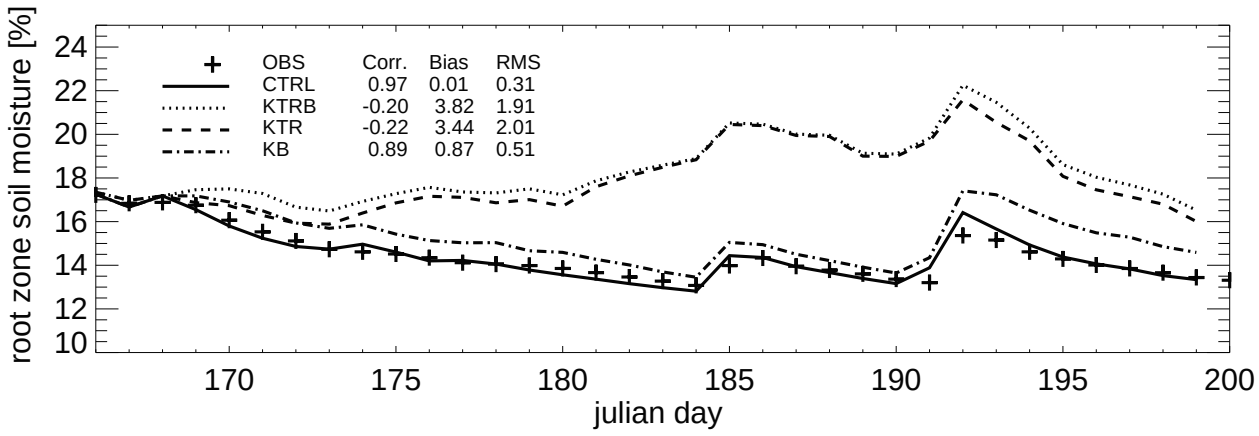

Figure 8: Temporal evolution for 15.6 – 19.7.1997 of daily mean volumetric root zone soil moisture [%] simulated by the ctrl-, KTR-, KB- and KTRB-run in comparison with observation from SGP97.

When the idealized forcing conditions are perturbed by setting precipitation to zero for the whole period, the soil moisture in the Ctrl-run dries until the wilting point is reached (Fig. 9a+b). The KTR-run is only slightly affected with regard to simulated root zone soil moisture because the soil moisture evolution is dominated by the period when soil moisture is used as a tuning parameter to compensate for deficiencies in the model (Fig. 9a). In the surface layer the KTR-run only slightly increases soil moisture confirming that the EKF system puts more weight on the second and third soil layer (Fig. 9b). However, the assimilation of T_B recovers surface and root zone soil moisture, when data are available (Fig.9a+b). This results agrees with the finding by Calvet and Noilhan (2000), who have shown that T_B observation every 3 days are sufficient to restore soil moisture. When all three observation types are assimilated the surface soil moisture is dominated by the assimilation of T_B. These results show that the assimilation of T_B additionally to T_{2m} and RH_{2m} helps to improve especially surface soil moisture, which is underestimated in the EKF analysis system based on T_{2m} and RH_{2m}.

5.2.4 Fit to observed surface energy fluxes

Despite the fact that the assimilation of T_{2m} and RH_{2m} deteriorate the simulated root zone soil moisture compared with the observations, simulated net radiation and energy fluxes (H, LE) of the KTR, KTRB, KB runs are in better agreement with the observations than the Ctrl-run (Fig. 10a-c). This indicates that soil moisture is used to compensate for other deficiencies in the experiment setup (section 5.2.3) but leads to improved simulation of the atmospheric state. For both latent and sensible heat fluxes the bias is reduced by up to 32 and 24W/m^2, respectively, in the assimilation runs and the correlation and root mean square errors are also improved (Fig. 10b+c). The best results are achieved with the synergy of screen-level parameters and T_B, because one observation type compensates the lack of the other. For the ground heat flux the Ctrl-run gives better results than KTR-, KB- and KTRB-runs compared with the measurements, though the differences are negligible (not shown).
The bias in the net radiation for all four model runs can be explained by the use of simulated down-welling longwave radiation in the SCM forcing (see section 4.1.2) and differences between observed and simulated surface temperature. The assimilation of all three parameters leads to a better agreement of net radiation because the reduced simulated surface temperatures in these runs lead to lower outgoing longwave radiation.
Figure 11 shows the daytime (6-18 LST) mean evaporative fraction, defined as $\frac{LE}{LE+H}$. The observed evaporative

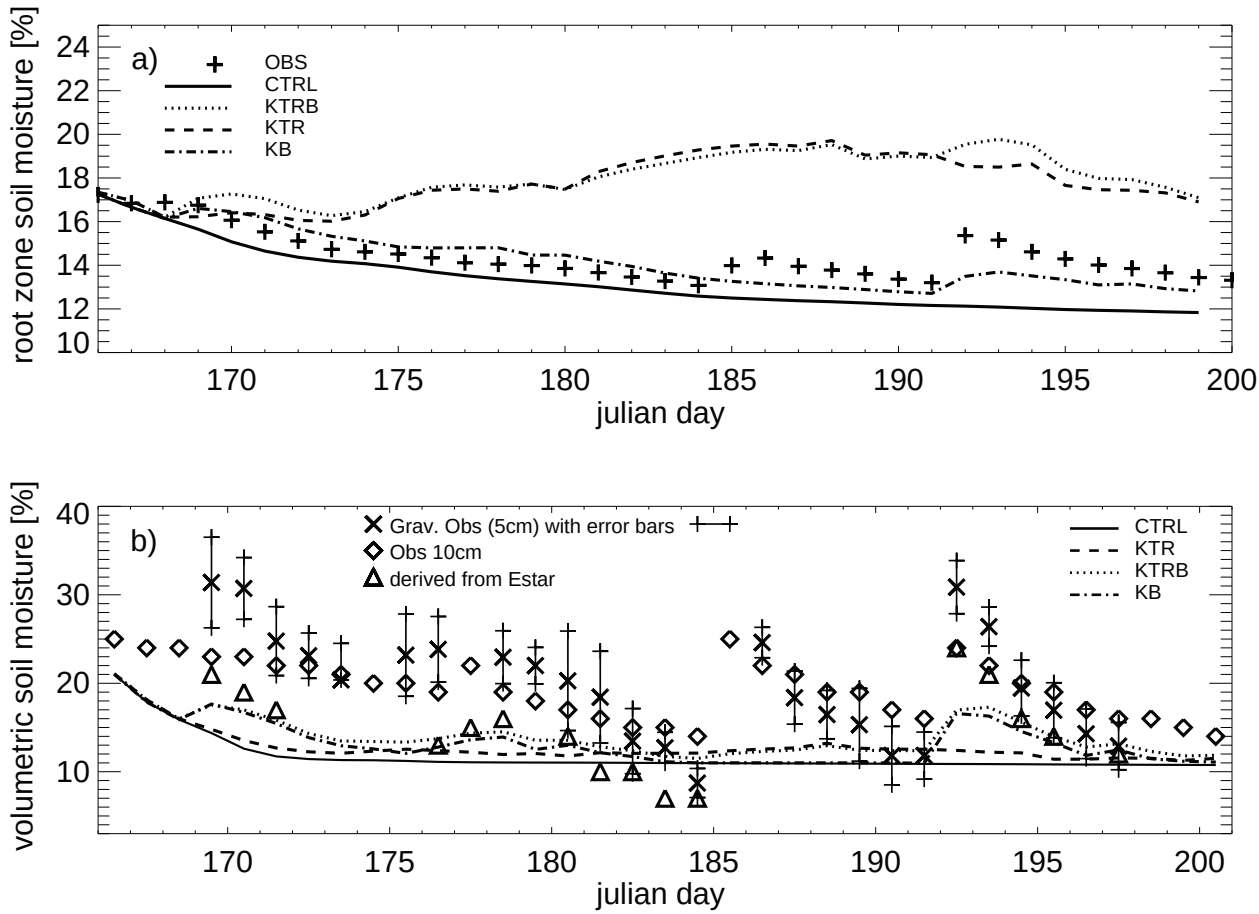

Figure 9: Temporal evolution for 15.6 – 19.7.1997 of a) root zone soil moisture and b) surface soil moisture simulated by the ctrl-, KTR-, KB- and KTRB-run with perturbed forcing (Precipitation set to zero) in comparison with observations from SGP97.

fraction shows only slight day by day variations with a minimum value of 0.55 and maximum value of 0.73 for the whole period. In contrast the simulated evaporative fraction of the Ctrl run varies substantially (min value of 0.25, max value of 0.76). These day by day variations of simulated evaporative fraction are reduced in the KB and especially in KTR- and KTRB-runs.

6 Discussion and conclusions

In current NWP-models imperfect parameterization of land surface interaction and cloud and precipitation processes may lead to considerable drifts in soil moisture and errors in the surface fluxes. To prevent these drifts soil moisture can be adjusted by assimilating observations of screen-level parameters or T_B. Screen-level parameters contain a signal of the underlying root zone soil moisture in weather situations with a strong solar forcing whereas T_B observations provide more direct information of the near surface soil moisture. In an operational NWP context, T_{2m} and RH_{2m} are currently assimilated based on OI or a simplified EKF analysis system, where the EKF system has the advantage of a dependence of forecast errors on the weather regime and also

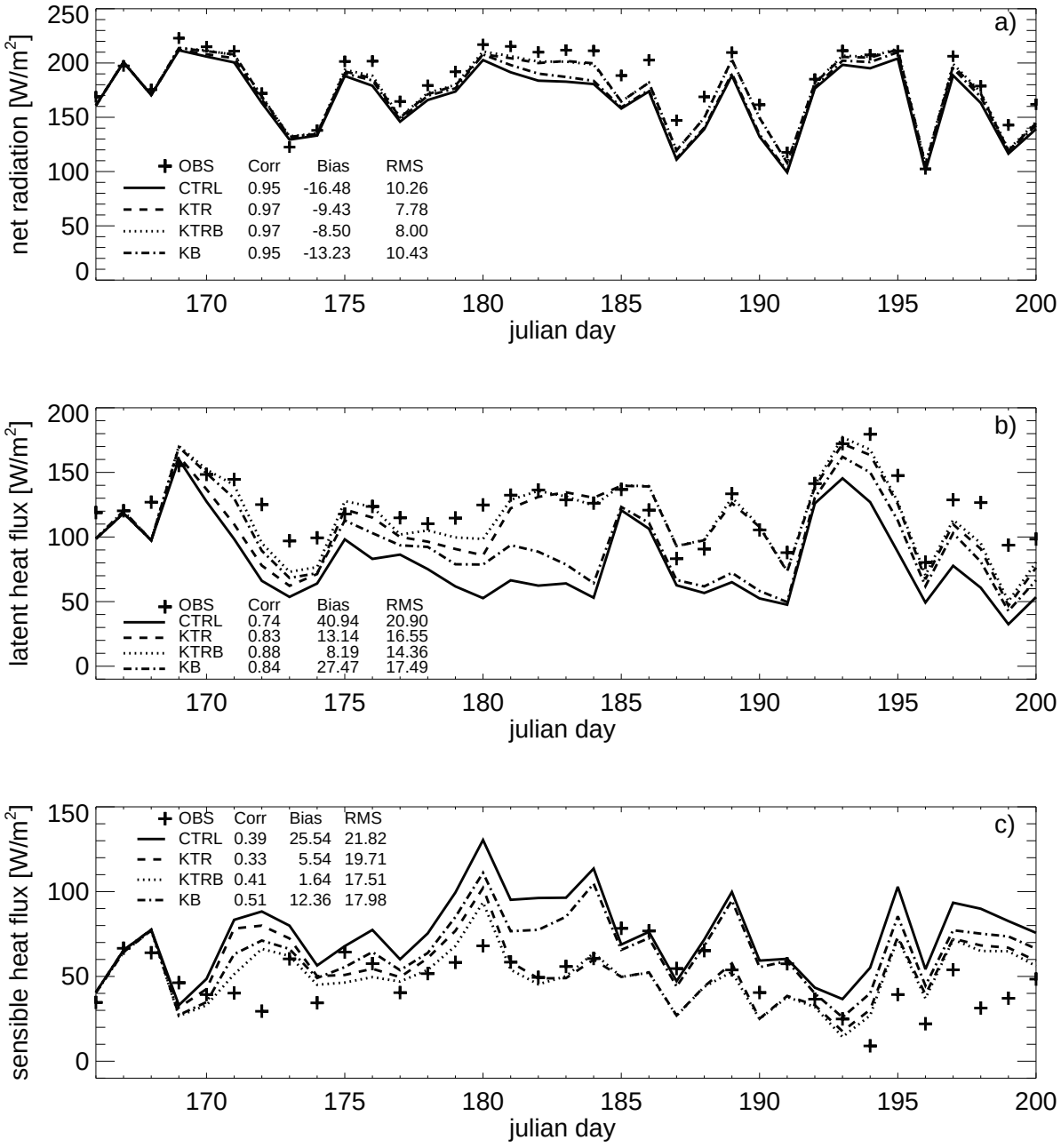

Figure 10: Temporal evolution for 15.6 – 19.7.1997 of daily mean a) net radiation, b) latent heat flux and c) sensible heat flux simulated by the ctrl-, KTR-, KB- and KTRB-run in comparison with observations from SGP97.

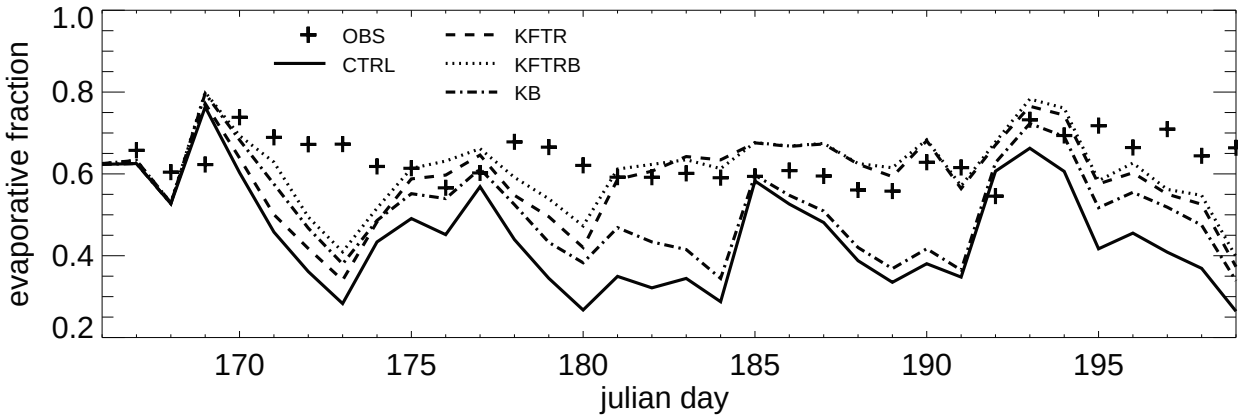

Figure 11: Temporal evolution for 15.6 – 19.7.1997 of daytime mean evaporative fraction simulated by the ctrl-, KTR-, KB- and KTRB-run in comparison with observation from SGP97.

allows for an easier inclusion of new observation types and the use of data from asynoptic times.
In this study the performance of OI and EKF for soil moisture analysis and the potential of soil moisture analysis based on screen-level parameters in combination with remotely sensed 1.4 GHz T_B observations has been explored.
(i) The OI and EKF method are compared using FIFE 1987 data, giving similar results compared with observed gravimetric soil moisture and surface heat fluxes. The OI system produces soil moisture increments of similar magnitude for the three soil layers whereas in the EKF method they increase from the first to the third layer. The overall water added to the soil due to the analysis is slightly larger in the EKF system compared with the OI system. This leads to a slightly better simulation of the observed hydrological budget with EKF than with OI system. The temporal evolution of the the gain matrix is almost the same for both systems. Though the simulated results are similar for both systems, the EKF method can be regarded as superior, because it does not require ad-hoc atmospheric criteria to account for special weather conditions. The OI system is almost fixed to perform the assimilation at 06, 12 and 18 LST whereas the EKF system is more flexible in the temporal choice of assimilated parameters. It especially allows for the easy use of data from asynoptic times. Hence, screen-level parameters can be chosen at observation times where the soil-atmosphere feedback is supposed to be maximal (e.g 09, 12, 15 LST) and T_B measurements can be easily incorporated from any available time. A drawback of the EKF method is that it requires more computer time than the OI method because of additional forecast runs. Nevertheless, it is still feasible to use EKF in operational weather forecasts (Hess, 2001).
(ii) To investigate whether the assimilation of different observations types improves the simulation, model runs with different combinations of T_{2m}, RH_{2m} and T_B are compared with independent observations for SGP97. The model runs are conducted with either perfect forcing or forcing with precipitation set to zero. The EKF system is used in this investigation because it offers an easier implementation of new observation types. In general the assimilation of T_{2m}, RH_{2m} or/and T_B leads to a better agreement of observed and simulated energy fluxes compared with a control run without any data assimilation. The imposed soil moisture increments for the second and third layer are smaller when T_B is assimilated, because the analysis has to transport the surface soil moisture signal to the other two layers, whereas T_{2m} and RH_{2m} directly include information of these layers. Conversely, the EKF-system based on T_{2m} and RH_{2m} only underestimates soil moisture increments of the first soil layer, which is especially shown when the forcing was perturbed (precipitation set to zero). When both types of observations are assimilated, the soil moisture analysis is dominated by the screen-level parameters with their indirect signal of the whole root zone although the observation error for T_B has been prescribed to

a small value. But the additional assimilated surface soil moisture information obtained by the T_B observation leads to additional corrections of the surface and root zone soil moisture and hence atmospheric parameters. Conversely, in cases when T_B is not available every day or irregularly sampled, the addition of screen-level parameters results in better simulated atmospheric parameters.
This case study also illustrates potential problems in the use of screen-level parameters for soil moisture analysis. During a ten day period simulated soil moisture is used as a tuning parameter to compensate for deficiencies in the model, that are not related to soil moisture. In this case the soil moisture analysis still leads to an improvement of simulated energy fluxes but at the expense of a deterioration of root zone soil moisture compared with observations (sections 5.2.3/5.2.4, Fig. 8, 10,11). In NWP frameworks it is useful to apply soil moisture analysis based on T_{2m} and RH_{2m} in these cases because correct specifications of the flux conditions are needed by the atmospheric model. In hydrological applications, in which correct soil moisture is important, the use of screen-level parameters for soil moisture analysis has to be treated with greater caution.
However, the simplified EKF system offers a tool to easily assimilated different observation types and the synergy of screen-level and 1.4 GHz T_B leads to more consistent results in a NWP framework. The potential of assimilating different data types could also be tested with 6.9 GHz T_B where the AMSR-E instrument already offers the possibility of a global data set. In future, for this application also 1.4 GHz observation might become available with the ESA SMOS mission.
In contrast to the atmosphere, land surface processes and the coupling to the atmosphere are inaccurately represented in current state-of-the art NWP models, which lead to problems in the background fields for the assimilation. The inclusion of new observation types (like Tb, surface heating rates, biomass) for land surface analysis will expose deficiencies in the background model suggesting directions for improvements. Until the land surface model are significantly improved the use of bias correction procedures will be a necessity. Therefore, the inclusion of new observations in soil moisture data assimilation will not only improve the quality of the analyzed soil moisture but also in the longterm increase the realism of the land surface model.

Acknowledgments

The work was supported by the European Commissions 5th framework programme on Energy, Environment and Sustainable Development (EVG1-CT-2001-00050) through the European Land Data Assimilation project. It was partly funded by the German Climate Research Program DEKLIM (01LD0006). The authors wish to thank Tilden P. Meyers from the NOAA Atmospheric Turbulence and Diffusion Division for making available the Little Washita flux station data and kindly answering questions about this data set. The SGP97 dataset were taken from: http://daac.gsfc.nasa.gov/CAMPAIGN_DOCS/SGP97/sgp97.html. The work benefited from valuable discussions with Anton Beljaars and Mike Fisher (ECMWF).

7 References

Balsamo, G., 2003: Analysis of soil moisture in a mesoscale weather prediction model, Univerisité Toulouse III -Paul Sabatier and University of Genoa, Météo-France/CNRM/GMAP 42, Av Coriolis 31057, Toulouse, France, 166p

Bélair, S., L.-P. Crevier, J. Mailhot, B. Bilodeau and Y. Delage, 2003: Operational implementation of the ISBA land surface scheme in the Canadian regional weather forecast model. Part I: Warm season results, J. Hydrometeor., 4, 352-470

Beljaars, A.C.M., and P. Viterbo, 1998: The role of the boundary layer in a Numerical Weather Prediction model. ”Clear and Cloudy Boundary Layers”, A.A.M. Holstlag and P.G. Duynkerke, Eds, 287-304. Royal Netherlands Academy of Arts and Sciences

Betts, A.K. and J.H. Ball, 1998: FIFE surface climate and site-average dataset 1987-1989. J. Atmos. Sci., 55, 1091-1108.

Calvet, J.-C. and J. Noilhan, 2000: from near-surface to root zone soil moisture using year-round data, J. Hydrometeor. Vol. 1, No. 5, 393-411

Choudhury, B.J., T.J. Schmugge and T. Mo, 1982: A Parameterization of effective soil temperature for microwave emission, J. Geophys. Res. Lett., 87, C2, 1301-1304.

Crow, W.T., M. Drusch and E.F. Wood, 2001: An observation system simulation experiment for the impact of land surface heterogeneity on AMSR-E soil moisture retrieval, IEEE Trans. Geo. Rem. Sens., 39 (8), 1622 - 1631

Crow, W.T., and E.F. Wood, 2003: The assimilation of remotely sensed soil brightness temperature imagery into land surface model using Ensemble Kalman filtering: a case study based on ESTAR measurements during SGP97. Advances in Water Resources, 26, 137-149

Dobson, M.C., F.T. Ulaby, M.T. Hallilainen and M.A. El-Rayes, 1985: Microwave dielectric behavior of wet soil -PartII: Dielectric Mixing Models, IEEE Trans. Geosci. Remote Sens., GE-23, 1, 35-46

Douville, H., P. Viterbo, J.-F. Mahfouf, and A.C.M. Beljaars, 2000: Evaluation of the Optimum Interpolation and Nudging techniques for soil moisture analysis using FIFE data, Month. Weath. Rev., 128, 1733-1756.

Drusch, M., R. Lindau and E.F. Wood, 1999: The impact of the SSM/I antenna gain function on land surface parameter retrieval, Geophys. Res. Let., 26, 3481 - 3484

Drusch, M., E.F. Wood, T.J. Jackson, 2001: Vegetative and atmospheric corrections for the soil moisture retrieval from passive microwave remote sensing data: results from the Southern Great Plains Hydrology Experiment 1997, J. Hydrometeor., 2, 181-192

Fisher, M., 2002: personal communication, ECMWF, Shinfield Park, Reading, RG2 9AX, U.K.

Fouquart, Y., and B. Bonnel, 1980: Computations of solar heating of the earth’s atmosphere: a new parameterization. Beitr. Phys. Atmosph., 53, 35-62

Gao, H., E.F. Wood, M. Drusch, W. Crow, T.J. Jackson, 2003: Using a microwave emission model to estimate soil moisture from ESTAR observations during SGP99, submitted to J. Hydromet.

Giard D. and E. Bazile, 2000: Implementation of a new assimilation scheme for soil and surface variables in a global NWP model, Month. Weath. Rev., 128, 997-1015.

Gregory, D., J-J. Morcrette, C. Jakob, A.C.M. Beljaars, and T. Stockdale, 2000: Revision of convection, radiation and cloud schemes in the ECMWF Integrated Forecasting System. Quart. J. Roy. Meteor. Soc., 126, 1685-1710

Hess, R., 2001: Assimilation of screen-level observations by variational soil moisture analysis. Meteorol. Atmos. Phys., 77, 145-154.

Jackson, T.J., D.M. Le Vine, A.Y. Hsu, A. Oldak, P.J. Starks, C.T.Swift, J.D. Isham and M. Haken, 1999: Soil moisture mapping at regional scales using microwave radiometry: The Southern Great Plains Hydrology Experiment. IEEE Trans. Geosci. Remote Sens., 37,2136-2150

Jakob, C., and S.A. Klein, 2000: A parameterization of the effects of cloud and precipitation overlap for use in General Circulation Models. Quart. J. Roy. Meteor. Soc., 126C, 2525-2544

Jones, A.S., I.C. Guch and T.H. Vonder Haar, 1998a: Data Assimilation of satellite-derived heating rates as proxy surface wetness data into a regional atmospheric mesoscale model. Part I: Methodology. Mon. Weath. Rev., 126, 634-645

Jones, A.S., I.C. Guch and T.H. Vonder Haar, 1998b: Data Assimilation of satellite-derived heating rates as proxy surface wetness data into a regional atmospheric mesoscale model. Part II: A case study. Mon. Weath. Rev., 126, 646-667

Joseph, J.H., W.J. Wiscombe, and J.A. Weinman, 1976: The delta-Eddington approximation for radiative flux transfer, J. Atm. Sci, 33, 2452-2459

Kerr, Y.H. and E.G. Njoku, 1990: A semiempirical model for interpreting microwave emission from semiarid land surfaces as seen from space, IEEE Trans. Geosc. Rem. Sens. 28, 384-393

Kerr, Y.H., P. Waldteufel, J.-P. Wigneron, J.-M. Martinuzzi, J. Font, and M. Berger, 2001: Soil moisture retrieval from space: the Soil Moisture and Salinity (SMOS) mission. IEEE Trans. Geosci. Remote Sens., 39, 1729-1735.

Kirdyashev, K.P., A.A. Churkhlantsev and A.M. Shutko, 1979: Microwave radiation of the Earth's surface in the presence of vegetation cover. Radio. Eng. Electron, 24, 256-64.

Klein, L.A. and C.T. Swift, 1977: An improved model for the dielectric constant of sea water at microwave frequencies, IEEE Trans. Ant. Prop., 25, 104-111

Le Vine, D.M., A.J. Griffis, C.T. Swift, and T.J. Jackson, 1994: ESTAR: A synthetic aperture microwave radiometer for remote sensing applications, Proc. IEEE, 82, 1787-1801

Liebe, J., 1989: MPM - An atmospheric millimeter-wave propagation model. Int. J. Infrared & Millimeter-waves, 10, 631-650

Mahfouf, J.F., 1991: Analysis of soil moisture from near-surface parameters. A feasibility study. J. Appl. Meteorol., 7, 506-526

Margulis, S.A., D. McLaughlin, D. Entekhabi, and S. Dunne, 2002: Land data assimilation and estimation of soil moisture using measurements from the Southern Great Plains 1997 field experiment. Water Resour. Res., 38(12),1299,doi:10.1029/2001WR001114.

Margulis, S.A. and D. Entekhabi, 2003: Variational assimilation of radiometric surface temperature and screen-level micrometeorology into a model of the atmospheric boundary layer and land surface. Mon. Wea. Rev., 131, 1272-1288.

McNider R.T., A.J. Song, D.M. Casey, P.J. Wetzel, W.L. Crosson and R.M. Rabin, 1994: Toward a dynamic-thermodynamic assimilation of satellite surface temperature in numerical atmospheric models. Mon. Wea.. Rev., 122, 2784-2803.

Meyers, T.P., 2001: A comparison of summertime water and $C0_2$ fluxes over rangeland for well watered and drought conditions. Agricult. Forest Meteorol., 106, 205-214.

Meyers, T.P.,2003: Personal communication, NOAA Atmospheric Turbulence and Diffusion Division, 456 S. Illinois Ave., Oak Ridge, TN 37830.

Mlawer, E.J., S.J. Taubman, P.D. Brown, M.J. Iacono, and S.A. Clough, 1997: Radiative transfer for inhomogeneous atmospheres: RRTM, a validated correlated-k model for the longwave. J. Geophys. Res., 102D,

16,663-16,682

Mölders N. and A. Raabe, 1997: Testing the effect of a two-way coupling of a meteorological and a hydrologic model on the predicted local weather. J. Atmos. Res., 45, 81-107.

Morcrette, J.-J., 2002: Assessment of ECMWF model cloudiness and surface radiation fields at the ARM SGP Site. Mon. Wea. Rev.,130,257-277.

Reichle, R.H., D. Entekhabi, and D.B. McLaughlin, 2001: Downscaling of radiobrightness measurements for soil moisture estimation: A four-dimensional variational data assimilation approach. Water Resour. Res., 31,2353-2364

Reichle, R.H., D.B. McLaughlin, and D. Entekhabi, 2002: Hydrologic data assimilation with the Ensemble Kalman filter. Mon. Wea. Rev., 130, 103-114

Rhodin A., F. Kucharski, U. Callies, D.P. Eppel and W. Wergen, 1999: Variational soil moisture analysis from screen-level atmospheric parameters: Application to a shortrange weather forecast model. Q.J.R. Met. Soc., 125, 2427-2448

Seuffert, G., P. Gross, C. Simmer and E.F. Wood, 2002: The influence of hydrologic modeling on the predicted local weather: Two-way coupling of a mesoscale weather prediction model and a land surface hydrologic model. J. Hydrometeor., Vol.3, No.5, 505-523.

Seuffert, G., H. Wilker, P.Viterbo, J.-F. Mahfouf, M. Drusch and J.-C. Calvet, 2003: Soil moisture analysis combining screen-level parameters and microwave brightness temperature: A test with field data, submitted to Geophys. Resear. Let.

Tiedtke, M., 1989: A comprehensive massflux scheme for cumulus parameterization in large-scale models. Mon. Wea. Rev., 117, 1779-1800

Tiedtke, M., 1993: Representation of clouds in large-scale models. Mon. Wea. Rev., 121, 3040-3061

Ulaby, F.T., M. Razani, and M. Dobson, 1983: Effects of vegetation cover on the microwave radiometric sensitivity to soil moisture, IEEE Trans. Geosci. Remote Sens., Ge-21, 1, 51-61.

van Genuchten, M. Th., 1980: A closed-form equation for predicting the hydraulic conductivity of unsaturated soils. Soil Sci. Soc. Am. J., 44, 892-898

van den Hurk, B.J.J.M., P. Viterbo, A.C.M. Beljaars, and A.K. Betts, 2000: Offline validation of the ERA40 surface scheme . ECMWF Tech. Mem. 295, 42pp.

van den Hurk, B.J.J.M. and H. The, 2002: Assimilation of satellite derived surface heating rates in a Numerical Weather Prediction model. Scientific report WR-2002-04, KNMI

Viterbo, P. and A.C.M. Beljaars, 1995: An improved land surface parameterization scheme in the ECMWF model and its validation. J. Climate, 8, 2716-2748

Wang, J.R., and T.J. Schmugge, 1980: An empirical model for the complex dielectric permittivity of soils as a function of water content. IEEE Trans. on Geosci. and Remote Sensing, GE-18, 288-295.

Wang, J.R., and B.J. Choudhury, 1981: Remote sensing of soil moisture content over bare field at 1.4 GHz frequency, J. Geophys. Res., Vol 86, No. C6, 5277-5282

Wegmüller U. and C. Mätzler and E. Njoku, 1995: Canopy opacity models, *in* Passive microwave remote sensing of land-atmosphere interactions, VSP, Utrecht, The Netherlands, 375-387

Wegmüller, U. and C. Mätzler, 1999: Rough bare soil reflectivity model, IEEE Trans. Geosc. Rem. Sens., 37,

1391-1395

Wetzel, P.J., and D. Atlas and R.H. Woodward, 1984: Determining soil moisture from geosynchronous sateliite infrared data: A feasibility study. J. Climate and Appl. Meteor., 23, 375-391.

Wilheit, T.T., 1978: Radiative transfer in a plane stratified dielectric, IEEE Trans. Geosc. Rem. Sens. 16, 138-143.